processes

MDPI

Article

Modeling a Strain and Piezo Potentials in an InAs/GaAs Quantum Dot

Igor Filikhin [1,*], Branislav Vlahovic [1], Tanja Zatezalo [1], Abdennaceur Karoui [2] and Jimmie Oxley [3]

[1] Centers of Research Excellence in Science and Technology (CREST), Mathematics and Physics Department, North Carolina Central University, Durham, NC 27707, USA; vlahovic@nccu.edu (B.V.); tzatezal@nccu.edu (T.Z.)
[2] Department of Mathematics, Computer Science, & Engineering Technology, Elizabeth City State University, Elizabeth City, NC 27909, USA; abkaroui@ecsu.edu
[3] Department of Chemical Engineering, University of Rhode Island, Kingston, RI 02881, USA; joxley@chm.uri.edu
* Correspondence: ifilikhin@nccu.edu

Abstract: We investigated the single-electron spectrum of an InAs/GaAs quantum dot (QD) using an effective potential model developed in previous studies. Our objective was to explore the limits of applicability of this model. We conducted numerical simulations, introducing a piezoelectric potential as a perturbation to the effective potential. The profile of this additional potential was derived from theoretical numerical studies presented in the literature. We analyzed the impact of variations in this profile within the framework of the perturbation theory. Our findings indicate that within a variation range of 25%, the effective potential model remains applicable.

Keywords: semiconductor quantum dots; strain potential; piezoelectric potential; effective model for InAs/GaAs heterostructures

Citation: Filikhin, I.; Vlahovic, B.; Zatezalo, T.; Karoui, A.; Oxley, J. Modeling a Strain and Piezo Potentials in an InAs/GaAs Quantum Dot. *Processes* **2024**, *12*, 2524. https://doi.org/10.3390/pr12112524

Academic Editor: Fang-Chung Chen

Received: 9 September 2024
Revised: 1 November 2024
Accepted: 11 November 2024
Published: 13 November 2024

1. Introduction

An InAs/GaAs quantum dot is a nanoscale semiconductor structure with unique properties arising from quantum confinement. It is created by embedding InAs within a GaAs substrate, leading to discrete energy levels and a range of applications in advanced electronic and optoelectronic devices.

Due to the lattice mismatch between InAs and GaAs [1], strain in InAs/GaAs heterostructures plays a crucial role in defining the material's electronic and optical properties and the functionality of nanostructured devices. As the lattice constant of InAs is larger than that of GaAs, when InAs is grown on GaAs, it leads to compressive strain in the InAs layer and tensile strain in the GaAs layer. This strain can affect the electron behavior in the heterostructure via the energy band structure and mobility.

The piezoelectric effect arises from the strain-induced polarization in the material, such as in III–V semiconductor heterostructures like InAs/GaAs. This effect can be significant due to the presence of both strain and the inherent piezoelectric properties of the materials. Strain modifies the energy band structure, leading to changes in the energy levels and carrier transport properties [2]. Additionally, the piezoelectric effect further influences the band structure by introducing an electric field due to strain-induced polarization. The induced electric field can affect the confinement of carriers in quantum structures and modify their energy levels. Overall, the interplay between strain and the piezoelectric effect in InAs/GaAs heterostructures is crucial for understanding and engineering their electronic and optoelectronic properties [3,4], making them essential in various device applications such as high-speed transistors, lasers, and quantum sensors and detectors [5].

In Ref. [6], the effective potential model was proposed to describe the confined states in quantum dots (QDs) and rings (QRs). The model was validated against reported

experimental data and used to further explore its applicability for explaining experimental data. In this work, we investigate the limits of applicability of this model. Variations in the effective potential induced by piezoelectric effects are applied to show the effect on the electron spectrum.

2. Theoretical Model

InAs/GaAs QDs have been modeled using the ***kp***-perturbation single sub-band effective mass approximation [6]. In that case, the single electron properties are formulated by the Schrödinger equation:

$$\left(\hat{H}_{kp} + V_c(r) + V_s(r)\right)\Psi(r) = E\Psi(r), \quad (1)$$

where $\hat{H}_{kp}$ is the single band ***kp***-Hamiltonian operator, $\hat{H}_{kp} = -\nabla\frac{\hbar^2}{2m^*}\nabla$; m^* is the electron effective mass, which depends on the radial position of the electron, and can thus be written as $m^*(r)$; and $V_c(r)$ is the band gap potential. The Ben Daniel–Duke boundary conditions [7] are defined at the interface of the QD material and the substrate. Here, we describe the confinement model proposed in Ref. [6] (also, see references in this publication) for the conduction band. Both the confinement potential $V_c(r)$ and the strain-induced potential $V_s(r)$ act inside the QDs; the latter is added to simulate the strain effect in the InAs/GaAs heterostructure. While V_s is "attractive", V_s is "repulsive" and reduces the strength of the electron confinement.

Inside QDs, the bulk conduction band offset is null since $V_c(r) = 0$, while it is equal to non-null constant V_c outside the QD. The band gap potential for the conduction band is fixed to $V_c(r) = 0.594$ eV [6]. The bulk effective masses of InAs and GaAs are $m_1^* = 0.024m_0$ and $m_2^* = 0.067m_0$, respectively, where m_0 is the free electron mass.

The magnitude of the effective potential $V_s(r)$ that simulates the strain effect is adjusted so that the results match the experimental data for the InAs/GaAs quantum dots. The adjustment depends mainly on the materials composing the heterojunction and, to a lesser degree, on the QD topology. For example, the magnitude of V_s for the conduction band chosen in Ref. [7] is 0.21 eV. This value was obtained to re-match the ab initio results obtained based on eighth band k.p calculations for InAs/GaAs QDs. The value of 0.31 eV was obtained from the experimental data reported by Lorke et al. [8]. The main advantage of using the effective potential is the simplicity of theoretical consideration and practically more efficient calculations for different nano-sized systems. The band-gap model described above is schematically presented in Figure 1a.

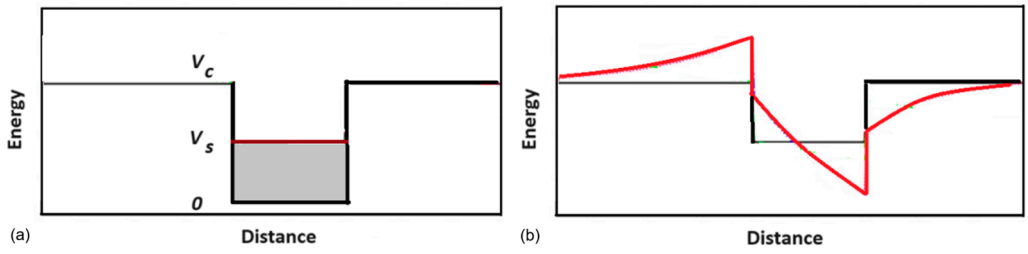

Figure 1. (**a**) A schematic representation of the potentials for the effective model. The confinement potential V_c (black lines) and the effective potential V_s (dark red line) are shown. (**b**) A schematic representation of the piezoelectric potential (red curves) calculated in Ref. [2].

The model is comparable with existing experimental data for InAs/GaAs heterostructures. In Ref. [6], an interpretation of C–V data has been proposed and compared to the study conducted by Lei et al. [8] on the basis of the oscillator model for a quantum ring (QR). Two geometry parameter sets were utilized to test the model regarding the reported self-assembled QR. The first is the experimental candidate for QR geometry, and the second is empirically deduced based on the oscillator model in connection to the model parameters and the quantum feature size. The additional energy of an electron in a magnetic field

was calculated with both geometries to match the C–V experimental data. It has been shown that the results of the calculation with the second geometry fit the experimental data rather well.

The effective approach similar to our effective model was presented by Califano and Harrison in the early paper [9].

3. Variations in Confinement and QD Geometry Model

The model proposed in the previous section can be validated through a "realistic" variation in parameters employing the piezoelectric potential calculated in the referenced literature. These calculations yield the profile depicted in Figure 1b. Notably, the potential exhibits a discontinuity along the interface boundary between the QD and the substrate.

We simulate the piezo-electric potential with piecewise continuous functions, as shown in Figure 2, where V_{p1} and V_{p4} potentials as well as V_{p2} and V_{p3} potentials have opposite signs to mimic the potential variation, as shown in Figure 1b. This scheme was realized in a three-dimensional model presented in Figure 3, with translation symmetry along the y-axis. For further simplification, the model was defined such that $V_p = |V_{p1}| = |V_{p2}| = |V_{p3}| = |V_{p4}|$. The results of the calculations are given in Figure 4.

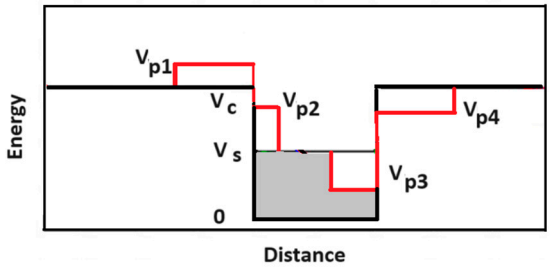

Figure 2. The variation in the effective model; the potential is approximated using the piecewise continuous functions. These enabled the simulation of calculations from Ref. [2] and Figure 1b. Here, V_{p1} and V_{p2} are positive values. V_{p3} and V_{p4} are negative values.

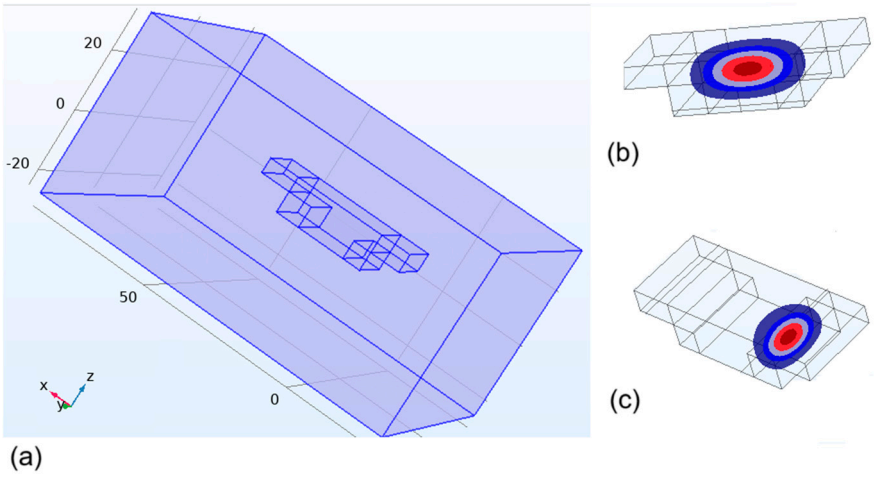

Figure 3. (**a**) The 3D geometry of the effective V_s potential, whose cross-sectional profile and defining parameters are shown in Figure 2. The scale is in nm. (**b**) The localization of the 3D wave function of the electron ground state in the QD when the unperturbed effective model $V_p = 0$ is applied. (**c**) The localization of the wave function of the electron ground state in the DQ when the perturbed effective model is applied with the parameter $V_p = |V_s/4|$.

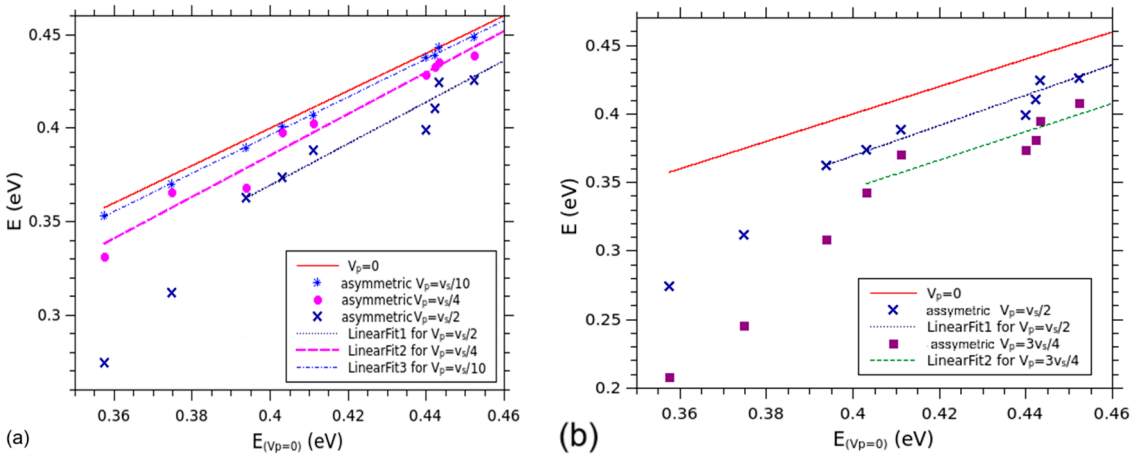

Figure 4. (**a**) A comparison of unperturbed (red line) and perturbed effective potential models (different cases are considered and represented with three types of dots). Small and intermediate values of the piezoelectric potential, $V_p = kV_s$, when $k < 0.25$, were considered. Linear fits of the data are shown. (**b**) The extreme values for the amplitude of the potential perturbations correspond to the case $k > 0.25$. The linear fits for the upper lying levels of the spectra are depicted (shown with dashed and dotted lines).

4. Numerical Results

We varied the piezo potential amplitude and calculated the spectrum of the electronic states in the QD for various geometries and potentials (see Figure 2). The amplitude V_p was scaled by the amplitude of the V_s potential, $V_p = kV_s$. We focused on two cases; the first one is related to small and intermediate values of piezoelectric potential and can be determined by the coefficient k from 0 and 0.25. This case is depicted in Figure 4a. When the potential has values $k > 0.25$, the typical nonlinear behavior of the spectrum fitting is shown in Figure 4b. The comparison of these two cases of the k value illustrates deviations from the initial linear-like spectrum distribution (when $V_p = 0$), presented as the red line in Figure 4. The distribution of the parts of the piezo-electric potential in the QD is asymmetrical, as shown in Figure 3.

The energy shift observed in the spectral deviations exhibits a linear behavior, depicted as parallel lines, with the same magnitude for all spectral levels when $k < 0.25$. Conversely, when $k > 0.25$, this regularity is disrupted. The lines develop irregularities, suggesting the presence of at least two distinct patterns.

5. Interpretation

The electron spectrum can be separated in two, namely "deep" and "normal" states. Figure 3b,c show the difference in these states. For the normal state, the wave function is located symmetrically over the QD volume. The "deep" state relates to the asymmetrical localization of the wave function within the quantum dot area that is deeper with more confinement energy. In other words, the deep negative part of the resulting effective potential generates a deeper electron state in a smaller volume compared to the regular case. In this case, the electron wave function is localized in such regions of the quantum dots, as shown in Figure 3c. Corresponding energies decrease, as shown in Figure 4. One can observe that the upper level exhibits a more uniform distribution, and the electron wave function is localized more evenly over the QD.

One can examine the resemblance between two presented models: the unperturbed model is defined by Equation (1), while the perturbed model includes an additional piezo-electric potential V_p. The connection between the two models is feasible when the coefficient k is within the range 0 to 0.25. Thus, the upper limit value can be chosen to formulate a limitation for the perturbation of the second model. The results of this comparison are depicted in Figure 5. The two models (differ by the amplitude of the potentials) lead to

similar results for the spectrum when the effective potential V_s becomes equal to 0.29 eV instead of the initial value of 0.31 eV. This situation is illustrated in Figure 5 with dotted and dashed lines. The lines are parallel, and the best matching can be obtained by fine-tuning the value of V_s.

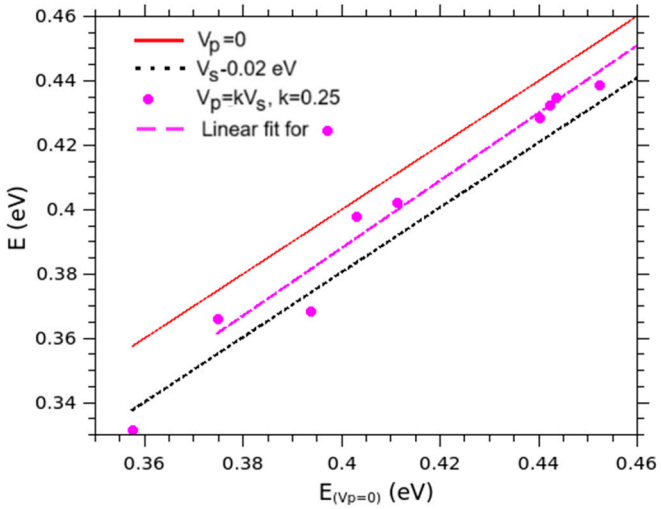

Figure 5. A comparison of the spectra for the unperturbed model, when $V_p = 0$ (red solid line), and the perturbed model with the additional piezoelectric potential, $V_p = kV_s$, $k = 0.25$, (solid circles). The adjustment value of the strain potential $V_s\prime = V_s - 0.02$ eV for the unperturbed model is shown with the dotted line. The dashed line calculated as fit to the results of the perturbed model. This fit does not take the ground state value into account.

6. Conclusions

The effective potential model was developed to describe electronic states in InAs/GaAs quantum dots. Within this model, the effective potential accounts for the strain and piezoelectric effects in the nanostructure in a phenomenological manner. This study evaluated the limit of the effective potential suitability, which was carried out by varying the effective potential incorporating a piezoelectric potential with an essential coordinate dependence. This potential was small and thus considered a perturbation to the effective potential model. We conducted simulations incorporating this additional piezoelectric potential, which closely mirrors the results of the realistic calculations outlined in Ref. [2], where we calculated the spectrum of the confinement states of the single electron. Our findings indicate that the effective model remains applicable for deviations in the effective potential up to 25%. Within such range, the model effectively captures variations in the strain and piezoelectric effects. In these studies, the effective potential was uniformly adjusted for all spectral states. However, a 25% increase in the magnitude of the additional potential may disrupt the initial spectrum structure. Note that the energy shifts for low-lying and upper-lying states differ due to the intricate dependence of the additional potential on the system's geometry coordinates. Specifically, this suggests that significant modifications are required for the effective potential model to accurately represent quantum dots composed of materials with strong piezoelectric properties. The strength of these properties may cause non-linarites in the potential that require more elaborate models.

Author Contributions: Conceptualization, B.V. and J.O.; methodology, I.F. and A.K.; software, I.F. and T.Z.; validation, I.F., A.K. and T.Z.; investigation, I.F., T.Z. and B.V.; resources, J.O.; data curation, I.F.; writing—original draft preparation, I.F.; writing—review and editing, B.V., A.K. and J.O.; visualization, T.Z.; supervision, B.V.; project administration, I.F.; funding acquisition, I.F. All authors have read and agreed to the published version of the manuscript.

Funding: This work is supported by the DHS Science and Technology Directorate Office of University Programs Summer Research Team Program for Minority Serving Institutions through an interagency

agreement between the U.S. Department of Energy (DOE) and DHS. ORISE is managed by ORAU under DOE contract number DE-SC0014664. All opinions expressed in this paper are the authors' and do not necessarily reflect the policies and views of DHS, DOE, or ORAU/ORISE. This work is partly supported by the US National Science Foundation HRD-1345219 award and the Department of Energy/National Nuclear Security Administration Award #NA0004112. A.K. is supported by the NSF DMR 2401243 award.

Data Availability Statement: The data are available upon request.

Acknowledgments: I.F. thanks A. Joseph for technical support.

Conflicts of Interest: The authors declare no conflicts of interest.

References

1. Schliwa, A.; Winkelnkemper, M.; Bimberg, D. Impact of size, shape, and composition on piezoelectric effects and electronic properties of In(Ga)As/GaAs quantum dots. *Phys. Rev. B* **2007**, *76*, 205324. [CrossRef]
2. Prabhakar, S.; Melnik, R. Influence of electromechanical effects and wetting layers on band structures of AlN/GaN quantum dots and spin control. *J. Appl. Phys.* **2010**, *108*, 064330. [CrossRef]
3. Voon, L.C.L.Y.; Willatzen, M. Electromechanical phenomena in semiconductor nanostructures. *J. Appl. Phys.* **2011**, *109*, 031101. [CrossRef]
4. Sladek, J.; Sladek, V.; Repka, M.; Pan, E. Size effect in piezoelectric semiconductor nanostructures. *J. Intell. Mater. Syst. Struct.* **2022**, *33*, 1351–1363. [CrossRef]
5. Ebeid, E.Z.M.; Okba, E.A. *Quantum Dots: Their Unique Properties and Contemporary Applications, in Advances in Semiconductor Physics, Devices and Quantum Dots*; Okba, E.A., Autran, J.-L., Yin, T., Munteanu, D., Eds.; InTech Open: Rijeka, Croatia, 2024. [CrossRef]
6. Filikhin, I.; Suslov, V.M.; Vlahovic, B. C-V Data and Geometry Parameters of Self-Assembled InAs/GaAs Quantum Rings. *J. Comput. Theor. Nanosci.* **2012**, *9*, 669–672. [CrossRef]
7. Ben-Daniel, D.J.; Duke, C.B. Space-Charge Effects on Electron Tunneling. *Phys. Rev.* **1966**, *152*, 683. [CrossRef]
8. Lorke, A.; Luyken, R.J.; Govorov, A.O.; Kotthaus, J.P.; Garcia, J.M.; Petroff, P.M. Spectroscopy of Nanoscopic Semiconductor Rings. *Phys. Rev. Lett.* **2000**, *84*, 2223–2226. [CrossRef] [PubMed]
9. Califano, M.; Harrison, P. Presentation and experimental validation of a single-band, constant-potential model for self-assembled InAs/GaAs quantum dots. *Phys. Rev. B* **2000**, *61*, 10959–10965. [CrossRef]